**D. Gregory[1], R. Large[1], S. Bull[1], J. Halpin[1], E. Lounejeva[1], V.V Maslennikov[2], P. Sack[3]**
[1] *ARC Centre of Excellence in Ore Deposit Research, University of Tasmania, Hobart, Australia, ddg@utas.edu.au*
[2] *Institute of Mineralogy UB RAS, Miass, Russia*
[3] *Yukon Geological Survey Whitehorse, Yukon, Canada*

## THE TRACE ELEMENT COMPOSITION OF SEDIMENTARY PYRITE AND VARIATIONS IN TRACE ELEMENT CONTENT WITH PYRITE TEXTURES

Изучение элементов-примесей в пирите осадочных толщ важно для понимания состава вод палеоокеана, особенностей соосаждения и диагенетического перераспределения металлов и полуметаллов в различных условиях. В статье обобщаются данные по составу примесей в пирите, полученные методом ЛА-ИСП-МС для 45 углеродистых сланцев от современных до архейского возраста. Показано, что примеси могут входить в структуру пирита и образовывать микровключения. Обычными примесями с содержаниями 100–1000 ppm являются As, Ni, Pb, Cu, Co; реже и в меньших количествах (10–100 ppm) встречаются Mo, Sb, Zn и Se; редко и в количествах до 10 ppm – Ag, Bi, Te, Cd, Au. Делается вывод о различии микропримесного состава диагенетических, метаморфогенных и гидротермальных пиритов в осадках.

The trace metal content of diagenetic pyrite is of interest for three main reasons: (1) it can be used to determine the chemical conditions of ancient oceans [Large et al., in prep.; Gregory et al., in prep.]; (2) it is a sink for metal and metalloid contamination in several environments [Huerta-Diaz and Morse, 1992; Lowers et al., 2007] and, (3) the trace metals within diagenetic pyrite can be remobilized to form ore deposits [Large et al., 2011; Large et al., 2009; Large et al., 2007; Thomas et al., 2011]. In this study diagenetic pyrite of several different textures was selected from 45 carbonaceous shale units of present to Archean age. These pyrites were then analyzed by LA-ICPMS to determine their trace metal content. The abundance of the trace metals can be split into 3 groups: most abundant, moderately abundant and least abundant. The most abundant elements are As, Ni, Pb, Cu and Co (median values ranging from 100 to 1000 ppm), the moderately abundant are Mo, Sb, Zn and Se (median values ranging from 10 to 100 ppm) and the least abundant are Ag, Bi, Te, Cd and Au (median values from 0.01 to 10 ppm) (Fig. 1). The data also showed that the trace metals are held within the pyrite in

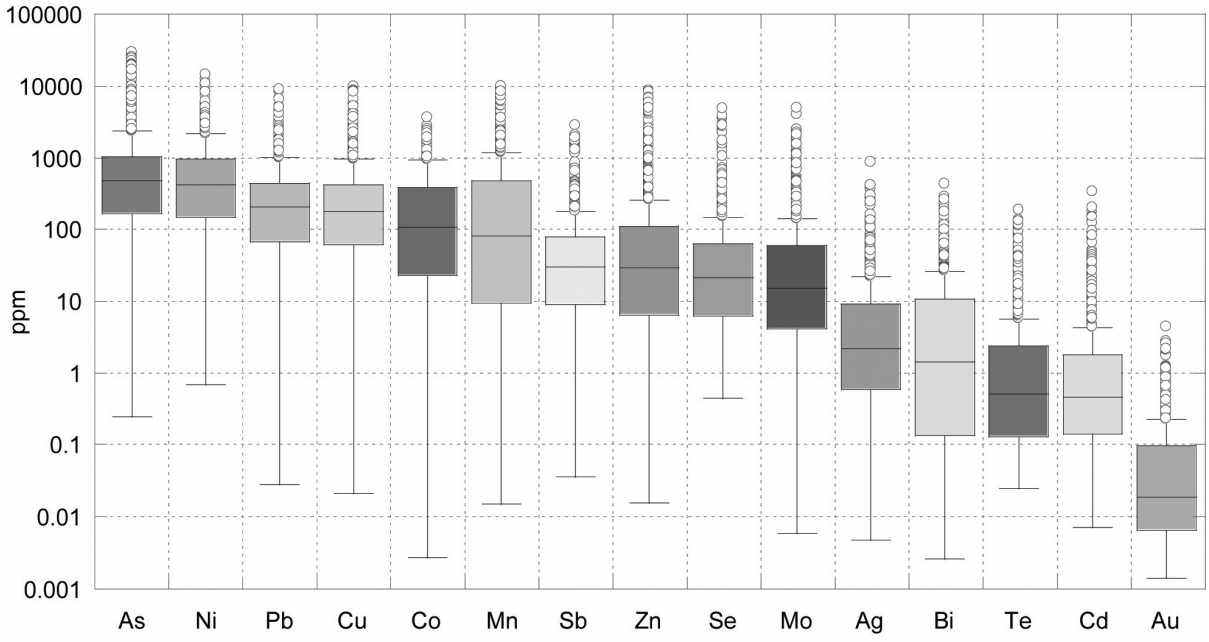


**Fig. 1.** Boxplot of trace metal content of pyrite in descending order of elemental abundance in pyrite: As ≥ Ni > Pb ≥ Cu ≥ Co ≥ Mn > Sb ≥ Zn ≥ Se ≥ Mo > Ag ≥ Bi > Te ≥ Cd > Au.

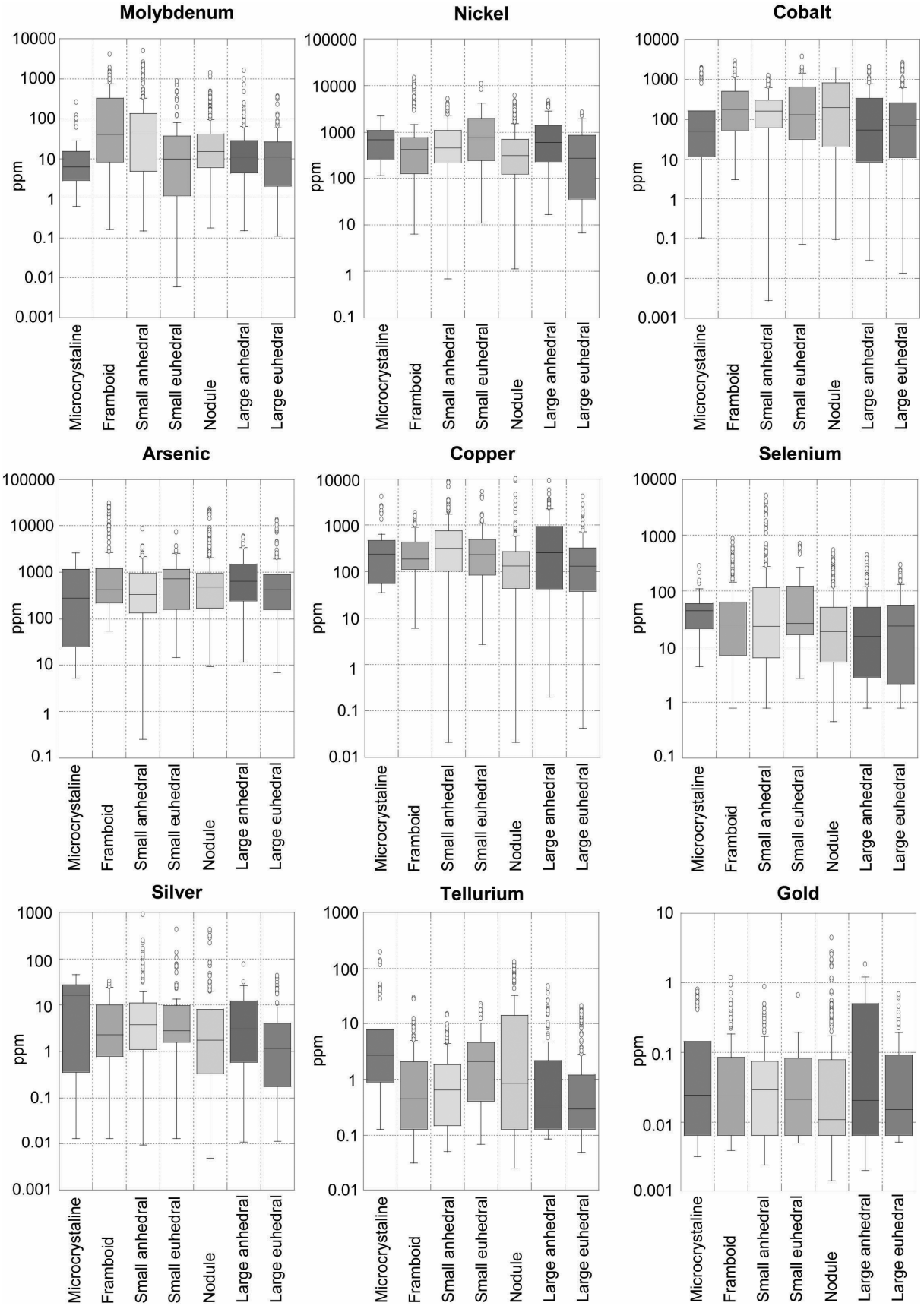


**Fig. 2.** Trace metal content of pyrite with groupings based on pyrite texture (microcrystalline, framboidal, small anhedral, small euhedral, nodule, large anhedral, large euhedral) for Mo, Ni, Co, As, Cu, Se, Ag, Te and Au.

*Table*

**Mean geochemical values for pyrite of different textures but from the same sample**

| Mount | Texture | n | Formation | Co | Ni | Cu | Zn | As | Se | Mo | Ag | Sb | Te | Au |
|---|---|---|---|---|---|---|---|---|---|---|---|---|---|---|
| 1 | Microcrystalline | 6 | Jet Rock | 75 | 401 | 103 | 122 | 328 | 9 | 100 | 2 | 7 | 1.5 | 0.04 |
| 1 | Nodule | 22 | Jet Rock | 48 | 238 | 61 | 51 | 272 | 7 | 108 | 1 | 3 | 1.2 | 0.02 |
| 2 | Framboid | 5 | Que River Shale | 297 | 511 | 252 | 128 | 764 | 77 | 20 | 17 | 85 | – | 0.20 |
| 2 | Nodule | 5 | Que River Shale | 100 | 287 | 221 | 46 | 304 | 118 | 1 | 8 | 43 | 0.7 | 0.10 |
| 3 | Microcrystalline | 14 | McRea Formation | 53 | 125 | 54 | 44 | 1194 | 21 | 8 | 0 | 18 | 0.9 | 0.03 |
| 3 | Nodule | 7 | McRea Formation | 2 | 21 | 212 | 3 | 338 | 3 | 1 | 1 | 22 | 0.7 | 0.04 |
| 4 | Microcrystalline | 5 | McRea Formation | 184 | 384 | 233 | 47 | 322 | 14 | 5 | 6 | 58 | 6.0 | 0.07 |
| 4 | Small anhedral | 3 | McRea Formation | 195 | 501 | 328 | 44 | 475 | 15 | 4 | 9 | 74 | 7.7 | 0.10 |
| 4 | Large euhedral | 10 | McRea Formation | 116 | 272 | 264 | 28 | 1111 | 17 | 4 | 3 | 36 | 4.3 | 0.05 |
| 5 | Small euhedral | 12 | Alum Shale | 137 | 2888 | 750 | 62 | 2204 | 205 | 332 | 55 | 123 | 3.0 | 0.08 |
| 5 | Nodule | 5 | Alum Shale | 88 | 2170 | 667 | 379 | 5696 | 405 | 200 | 323 | 228 | 5.8 | 0.43 |
| 6 | Framboid | 6 | Canol Formation | 77 | 1002 | 303 | 153 | 242 | 393 | 154 | 3 | 83 | 0.8 | 0.04 |
| 6 | Nodule | 8 | Canol Formation | 2 | 73 | 55 | 22 | 44 | 256 | 29 | 0 | 41 | 0.3 | 0.01 |
| 7 | Small euhedral | 6 | Warrabarty | 416 | 64 | 37 | 13 | 46 | 22 | 0 | 0 | 1 | 0.1 | 0.01 |
| 7 | Nodule | 10 | Warrabarty | 300 | 450 | 264 | 58 | 230 | 11 | 6 | 1 | 18 | 0.5 | 0.05 |
| 8 | Small anhedral | 9 | Yul-12005 | 87 | 524 | 2066 | 1355 | 160 | 42 | 208 | 7 | 20 | 1.9 | 0.04 |
| 8 | Large euhedral | 12 | Yul-12005 | 78 | 295 | 165 | 72 | 156 | 43 | 77 | 0 | 5 | 0.2 | 0.01 |

two ways; as micro-inclusions and incorporated into the structure of the pyrite. The different trace elements have thus been separated into 3 groups based on how the trace elements are incorporated into diagenetic pyrite. The first group consists of As, Ni, Co, Sb, Se and Mo and is held predominantly within the crystal structure of the pyrite. The second group consists of Ag, Au, Te and Cu, and is contained within the crystal structure of the pyrite at low concentrations but in micro-inclusions at high concentration. The final group is made up of Pb, Zn, Cd and Bi and is contained predominantly hosted in micro-inclusions within the pyrite.

Diagenetic pyrite generally contains enrichment in trace elements in the following order of abundance: As ≥ Ni > Pb ≥ Cu ≥ Co ≥ Mn > Sb ≥ Zn ≥ Se ≥ Mo > Ag ≥ Bi > Te ≥ Cd > Au. We have found that sedimentary pyrite has characteristic trace metal composition as follows: 0.01 < Co/Ni < 2, 0.01 < Cu/Ni < 10, 0.01 < Zn/Ni < 10, 0.1 < As/Ni < 10, Ag/Au > 2, 1 < Te/Au < 1000, Bi/Au > 1, Sb/Au > 100 and As/Au > 200. As hydrothermal and metamorphic pyrite have significantly different trace element compositions (Bajwah et al., 1987; Large et al., 2007) these chemical criteria can be used to determine whether pyrite is hydrothermal, metamorphic or sedimentary source when other methods to determining the pyrites origin are ambiguous.

The texture of diagenetic pyrite changes based on the local chemical conditions in which it forms, thus it is reasonable to expect that a difference in trace element concentrations in pyrite would also be observed. However, when the data set is taken as a whole this is not what is observed (Fig. 2). While there is some variation there is no systematic trend for higher or lower concentrations of pyrite within a given textural type. This suggests that other factors, such as depositional setting or age of pyrite, are more important controls in the trace element content of pyrite.

Although texture of diagenetic pyrite does not seem to be an important indicator of trace metal content over the entire data set it may be important in individual samples. Table shows the mean trace element content of pyrite of different textures for 8 samples that contain multiple pyrite textures. In the majority of the pyrite that was interpreted to have formed earlier (framboidal, microcrystalline, small anhedral and small euhedral) tends to have higher or equal trace metal content to the pyrite interpreted to have formed later. This is true for all textures except the fine euhedral. There are two possible reasons for this observation. First, the euhedral pyrite may have formed later than the nodules it is found with and the older pyrite (in this case the euhedral) contains fewer trace elements, which is similar to the rest of the data set. A second possibility is that the when the euhedral pyrite formed most of the trace elements were still adsorbed onto organic matter and other phases and were not free to be incorporated into the pyrite. Later during diagenesis the nodules formed by remobilizing sulphides in the surrounding shale [Ono et al., 2003]; trace elements were also remobilized and incorporated into the pyrite nodules.

*This research was supported by the projects CODES (Tasmania University, Australia) and UB of RAS (no. 12-II-5-1003).*

## References

*Bajwah, Z., Seccombe, P., and Offler, R.* Trace element distribution, Co:Ni ratios and genesis of the big cadia iron-copper deposit, New South Wales, Australia // Mineralium Deposita, 1987. Vol. 22. P. 292–300.

*Huerta-Diaz, M.A., Morse, J.W.* Pyritization of trace metals in anoxic marine sediments // Geochimica et Cosmochimica Acta, 1992. Vol. 56. P. 2681–2702.

*Large, R.R., Bull, S.W., and Maslennikov, V.V.* A carbonaceous sedimentary source-rock model for Carlin-type and orogenic gold deposits // Economic Geology, 2011. Vol. 106. P. 331–358.

*Large, R.R., Danyushevsky, L., Hollit, C., Maslennikov, V., Meffre, S., Gilbert, S., Bull, S., Scott, R., Emsbo, P., Thomas, H., Singh, B., and Foster, J.* Gold and Trace Element Zonation in Pyrite Using a Laser Imaging Technique: Implications for the Timing of Gold in Orogenic and Carlin-Style Sediment-Hosted Deposits // Economic Geology, 2011. Vol. 104. P. 635–668.

*Large, R.R., Maslennikov, V.V., Robert, F., Danyushevsky, L.V., and Chang, Z.S.* Multistage sedimentary and metamorphic origin of pyrite and gold in the giant Sukhoi Log deposit, Lena gold province, Russia // Economic Geology, 2007. Vol. 102. P. 1233–1267.

*Lowers, H.A., Breit, G.N., Foster, A.L., Whitney, J., Yount, J., Uddin, M.N., and Muneem, A.A.* Arsenic incorporation into authigenic pyrite, Bengal Basin sediment, Bangladesh // Geochimica et cosmochimica acta, 2007. Vol. 71. P. 2699–2717.

*Ono, S., Eigenbrode, J.L., Pavlov, A.A., Kharecha, P., Rumble, D., Kasting, J.F., and Freeman, K.H.* New insights into Archean sulfur cycle from mass-independent sulfur isotope records from the Hamersley Basin, Australia // Earth and Planetary Science Letters, 2003, Vol. 213. P 15–30.

*Thomas, H.V., Large, R.R., Bull, S.W., Maslennikov, V., Berry, R.F., Fraser, R., Froud, S., Moye, R.* Pyrite and pyrrhotite textures and composition in sediments, laminated quartz veins, and reefs at Bendigo gold mine, Australia: insights for ore genesis // Economic Geology, 2011. Vol. 106. P. 1–31.